

Is Self-Interference in Full-Duplex Communications a Foe or a Friend?

Animesh Yadav, *Member, IEEE*, Octavia A. Dobre, *Senior Member, IEEE*, and H. Vincent Poor, *Fellow, IEEE*

Abstract

This paper studies the potential of harvesting energy from the self-interference of a full-duplex base station. The base station is equipped with a self-interference cancellation switch, which is turned-off for a fraction of the transmission period for harvesting the energy from the self-interference that arises due to the downlink transmission. For the remaining transmission period, the switch is on such that the uplink transmission takes place simultaneously with the downlink transmission. A novel energy-efficiency maximization problem is formulated for the joint design of downlink beamformers, uplink power allocations and transmission time-splitting factor. The optimization problem is nonconvex, and hence, a rapidly converging iterative algorithm is proposed by employing the successive convex approximation approach. Numerical simulation results show significant improvement in the energy-efficiency by allowing self-energy recycling.

Index Terms

Small cells, full-duplex communications, self-interference, self-energy harvesting, radio resource management.

I. INTRODUCTION

Full-duplex (FD) transceivers can transmit and receive signals at the same time and frequency, and hence, provide improved spectral efficiency. However, the self-interference (SI), which suppresses the weak received signal of interest, limits their performance. With current SI cancellation (SIC) techniques, small power transceivers are identified as being suitable for FD deployment [1].

Recently, radio-frequency (RF) signals have been investigated for simultaneous wireless information and power transfer (SWIPT) [2]. Commonly, the RF signals' energy is harvested either by power- or time-splitting receivers. For the former (latter), the received signal power (transmission time) is divided into two parts: one used for information gathering and another one used for energy harvesting. Very recently, FD has been combined with SWIPT to boost both the spectral efficiency and energy efficiency (EE) of the system [3], [4]. Furthermore, the idea of self-energy (SEg) recycling from the SI is conceptualized in [5]–[7]. Both in [5] and [6], FD is used at the relay terminal and the time-splitting protocol is applied for the SEg harvesting. The system throughput is maximized in [5], whereas the signal-to-noise ratio (SNR) is maximized in [6]. In [7], the authors introduce a three-port circuit for recycling the SI and show significant improvement in the EE.

Since the SI carries high energy, it could potentially be harvested for some fraction of a total transmission time. Inspired from this idea, in this paper, we consider the SEg harvesting by the SI at a small cell base station (SBS). Particularly, we propose a time-splitting based two-phase protocol for SEg harvesting at the FD SBS. The SBS is equipped with an SIC switch: when it is turned-on, the SIC is activated; otherwise, SIC is disabled. In the first phase, the SIC switch is off and the SBS sends the *information-bearing* signal to its downlink (DL) users (UEs). The energy harvesting device at the SBS harvests the SI energy and also receives *energy-bearing* signals from its uplink (UL) UEs. In the second phase, the SIC switch is on, and no energy harvesting is possible from the residual SI signal. In this phase, the SBS continues to transmit the *information-bearing* signal to DL UEs and starts receiving the *information-bearing* signals from the UL UEs. We explore the optimal time-splitting factor that maximizes the EE of the system along with the optimal beamforming and power allocation design for the DL and UL UEs, respectively. Simulation results show the significant EE improvement offered by the proposed SEg harvesting scheme.

Notation: Bold uppercase and lowercase letters denote matrices and vectors, $(\cdot)^H$ and $(\cdot)^T$ represent the Hermitian and transpose operations, $|\cdot|$ and $\|\cdot\|_2$ denote the absolute value and ℓ_2 -norm, and $\text{tr}\{\cdot\}$ and $\mathbb{E}\{\cdot\}$ are used as the trace and expectation operators, respectively. \mathbf{I}_N represents the $N \times N$ identity matrix. $\mathbf{x}_{\geq y}$ represents a set where each element has value greater than y .

II. SYSTEM MODEL

We consider an FD SBS equipped with M_T transmit and M_R receive antennas, which serves K_D and K_U single antenna DL and UL UEs, respectively. The sets of DL and UL UEs are denoted by $\mathcal{D} = \{1, \dots, K_D\}$ and $\mathcal{U} = \{1, \dots, K_U\}$, respectively. The SBS is powered by a regular grid source, and is also equipped with an RF power harvesting device and a rechargeable

Copyright (c) 2017 IEEE. Personal use of this material is permitted. However, permission to use this material for any other purposes must be obtained from the IEEE by sending a request to pubs-permissions@ieee.org.

Animesh Yadav and Octavia A. Dobre are with Memorial University, St. John's, NL, A1B 3X9, Canada. (e-mail: {animeshy, odobre}@mun.ca).

H. Vincent Poor is with Princeton University, Princeton, NJ 08544 USA (e-mail: poor@princeton.edu).

battery for energy storage. We assume a flat fading channel model, in which all channels remain unchanged for a time block of duration T and change independently to new values in the next block.

The transmission time is divided into phases of duration αT and $(1 - \alpha)T$, where $\alpha \in (0, 1)$ is the time-splitting factor. In the first αT phase, the SBS transmits the *information-bearing* and receives the *energy-bearing* signals to and from the DL and UL UEs, respectively. The SIC switch in this phase is turned-off for SEg harvesting. Then, the received signal at the DL UE i is given by

$$y_{1,i}^{\text{D}} = \mathbf{h}_i^H \mathbf{w}_{1,i} s_i^{\text{D}} + \sum_{k \neq i}^{K_{\text{D}}} \mathbf{h}_i^H \mathbf{w}_{1,k} s_k^{\text{D}} + \sum_{j=1}^{K_{\text{U}}} g_{j,i} \sqrt{p_{1,j}} s_j^{\text{U}} + n_i^{\text{D}}, \quad (1)$$

where $\mathbf{w}_{1,i} \in \mathbb{C}^{M_T \times 1}$ and s_i^{D} with $\mathbb{E}\{|s_i^{\text{D}}|^2\} = 1$ are the beamforming vector and data of DL UE i , respectively; $p_{1,j}$ is the power coefficient allocated to the UL UE j during αT phase; the vector $\mathbf{h}_i \in \mathbb{C}^{M_T \times 1}$ and complex scalar $g_{j,i}$ denote the channel from the SBS to DL UE i and from the UL UE j to the DL UE i , respectively; and $n_i^{\text{D}} \sim \mathcal{CN}(0, \sigma_i^2)$ is complex additive white Gaussian noise (AWGN) at DL UE i , with variance σ_i^2 . The signal vector at the receive antennas of the SBS is given as

$$\mathbf{r} = \sum_{i=1}^{K_{\text{D}}} \mathbf{H}^H \mathbf{w}_{1,i} s_i^{\text{D}} + \sum_{j=1}^{K_{\text{U}}} \mathbf{g}_j \sqrt{p_{1,j}} + \mathbf{n}^r, \quad (2)$$

where $\mathbf{H} \in \mathbb{C}^{M_T \times M_R}$ and $\mathbf{g}_j \in \mathbb{C}^{M_R \times 1}$ are the SI channel matrix of the SBS and channel vector of UL UE j to the SBS, respectively; and $\mathbf{n}^r \sim \mathcal{CN}(\mathbf{0}, \sigma_r^2 \mathbf{I}_{M_R})$ is a complex AWGN vector at the receiver of the SBS. Consequently, the total SEg harvested at the SBS in the first phase is given by

$$E_{\text{H}} = \eta \alpha T \mathbb{E}\{|\mathbf{r}|^2\} = \eta \alpha T \left(\sum_{i=1}^{K_{\text{D}}} \|\mathbf{H}^H \mathbf{w}_{1,i}\|^2 + \sum_{j=1}^{K_{\text{U}}} p_{1,j} |\mathbf{g}_j|^2 \right), \quad (3)$$

where $\eta \leq 1$ represents the energy conversion efficiency of the harvester. In (3), the noise term is ignored as its contribution is negligible. In the second phase, the SBS turns the SIC switch on, which brings the SI power to the noise level. In this phase, the signals received at the DL UE i and SBS are, respectively, given as

$$y_{2,i}^{\text{D}} = \mathbf{h}_i^H \mathbf{w}_{2,i} s_i^{\text{D}} + \sum_{k \neq i}^{K_{\text{D}}} \mathbf{h}_i^H \mathbf{w}_{2,k} s_k^{\text{D}} + \sum_{j=1}^{K_{\text{U}}} g_{j,i} \sqrt{p_{2,j}} s_j^{\text{U}} + n_i^{\text{D}}, \quad (4)$$

$$\mathbf{y}_j^{\text{U}} = \mathbf{g}_j \sqrt{p_{2,j}} s_j^{\text{U}} + \sum_{l \neq j}^{K_{\text{U}}} \mathbf{g}_l \sqrt{p_{2,l}} s_l^{\text{U}} + \sum_{i=1}^{K_{\text{D}}} \mathbf{H}_{\text{on}}^H \mathbf{w}_{2,i} s_i^{\text{D}} + \mathbf{n}_j^{\text{U}}, \quad (5)$$

where $p_{2,j}$ and $\mathbf{n}_j^{\text{U}} \sim \mathcal{CN}(\mathbf{0}, \sigma_j^2 \mathbf{I}_{M_R})$ are the power coefficient allocated to UL UE j and the complex AWGN vector; and \mathbf{H}_{on} is the SI channel matrix, which captures the effect of SIC.

Using (1) and (4), the received signal-to-interference plus noise ratios (SINRs) at DL UE i in the first and second phases can be written as

$$\gamma_{l,i}^{\text{D}} = \frac{|\mathbf{h}_i^H \mathbf{w}_{l,i}|^2}{\sigma_i^2 + \sum_{k \neq i}^{K_{\text{D}}} |\mathbf{h}_i^H \mathbf{w}_{l,k}|^2 + \sum_{j=1}^{K_{\text{U}}} p_{l,j} |g_{j,i}|^2}, \quad (6)$$

where $l = 1, 2$ represents the phase. At the end of transmission time T , the achievable rate for DL UE i is given as $R_i^{\text{D}} = \alpha \log_2(1 + \gamma_{1,i}^{\text{D}}) + (1 - \alpha) \log_2(1 + \gamma_{2,i}^{\text{D}})$.

Next, for the UL transmission, using (5), the received SINR of UL UE j at the SBS, which applies the minimum-mean-squared error with successive interference cancellation receiver, is given by

$$\gamma_j^{\text{U}} = p_{2,j} \mathbf{g}_j^H \mathbf{X}_j^{-1} \mathbf{g}_j, \quad (7)$$

where $\mathbf{X}_j \triangleq \sigma_j^2 \mathbf{I}_{M_R} + \sum_{l > j}^{K_{\text{U}}} p_{2,l} \mathbf{g}_l \mathbf{g}_l^H + \sum_{i=1}^{K_{\text{D}}} \mathbf{H}_{\text{on}}^H \mathbf{w}_{2,i} \mathbf{w}_{2,i}^H \mathbf{H}_{\text{on}}$. Then, the achievable rate for UL UE j , at the end of transmission time T , is $R_j^{\text{U}} = (1 - \alpha) \log_2(1 + \gamma_j^{\text{U}})$.

Energy usage model: The combined energies consumed in the circuit and decoding operations are comparable or even dominate the actual transmit energy [8]. Consequently, these energies play a significant role in representing the total power consumption. Thus, the total power consumed at the SBS can be expressed as

$$P_b^{\text{con}} = \sum_{i=1}^{K_{\text{D}}} \frac{\alpha}{\epsilon} \|\mathbf{w}_{1,i}\|^2 + (1 - \alpha) \left(\frac{\|\mathbf{w}_{2,i}\|^2}{\epsilon} + \sum_{j=1}^{K_{\text{U}}} P_j^{\text{dec}}(R_j^{\text{U}}) \right) + P_b^{\text{cir}}, \quad (8)$$

where $\epsilon \in (0, 1)$ is the amplifier efficiency of the SBS; $P_b^{\text{cir}} = M_T P_{\text{rf}} + P_{\text{st}}$ is the total circuit power consumption, in which P_{rf} and P_{st} correspond to the active RF blocks, and to the cooling and power supply, respectively; and P_j^{dec} is the power consumption for data decoding of the UL UE j , which is a function of the achievable rate of the UE, i.e., for the UL UE j , $P_j^{\text{dec}}(R_j^{\text{U}}) = \beta_j R_j^{\text{U}}$ where β_j models the decoder efficiency, being decoder specific [8], [9].

Energy efficiency function: In the context of 5G networks, EE maximization is of paramount importance for both operators and users [10]. Thus, here as well our interest is to jointly optimize the DL UE beamformers, UL UE power coefficients and α such that the system EE is maximized. Unlike [10], we introduce a novel EE function that measures the efficiency

of the aggregated energies draw from the grid source at both SBS and UL UEs as $\eta(\mathbf{w}, \mathbf{p}, \alpha) \triangleq f(\mathbf{w}, \mathbf{p}, \alpha)/g(\mathbf{w}, \mathbf{p}, \alpha)$, where $f(\mathbf{w}, \mathbf{p}, \alpha)$ and $g(\mathbf{w}, \mathbf{p}, \alpha)$ capture the throughput and total grid energy consumed by the system, respectively. The sets \mathbf{w} and \mathbf{p} collect the optimization variables $\mathbf{w}_{1,i}$ and $\mathbf{w}_{2,i} \forall i \in \mathcal{D}$, and $\mathbf{p}_{1,j}$ and $\mathbf{p}_{2,j}, \forall j \in \mathcal{U}$, respectively. In particular, the throughput is given as $f(\mathbf{w}, \mathbf{p}, \alpha) = \sum_{i=1}^{K_D} R_i^D + \sum_{j=1}^{K_U} R_j^U$, and total grid power consumption is given as $g(\mathbf{w}, \mathbf{p}, \alpha) = P_b + P_u$. $P_b \triangleq \sum_{i=1}^{K_D} \alpha \|\mathbf{w}_{1,i}\|^2/\epsilon + \alpha P_b^{\text{cir}} + (1-\alpha)P_{2,b}$ denotes the consumption during the T period, with $P_{2,b}$ denoting the grid power consumed during the $(1-\alpha)T$ phase. $P_u \triangleq \sum_{j=1}^{K_U} \alpha p_{1,j} + (1-\alpha)p_{2,j}$ denotes the energy drawn from the battery source at the UL UEs during both the αT and $(1-\alpha)T$ phases.

III. ENERGY EFFICIENCY MAXIMIZATION

Using the notation introduced above, the constrained EE maximization problem is formulated as

$$\max_{\substack{\mathbf{w}, \mathbf{p}, \\ P_{2,b}, \alpha}} \eta(\mathbf{w}, \mathbf{p}, \alpha) \quad (9a)$$

$$\text{s.t. } R_j^U \geq \bar{r}_j^U \quad \forall j \in \mathcal{U}, \quad (9b)$$

$$\sum_{i=1}^{K_D} \alpha \|\mathbf{w}_{1,i}\|^2 + (1-\alpha) \|\mathbf{w}_{2,i}\|^2 \leq \bar{P}_b, \quad (9c)$$

$$\alpha p_{1,j} + (1-\alpha)p_{2,j} \leq \bar{P}_u \quad j \in \mathcal{U}, \quad (9d)$$

$$(1-\alpha) \left(P_b^{\text{cir}} + \sum_{j=1}^{K_U} \beta_j \log_2(1 + \gamma_j^U) \right) + \sum_{i=1}^{K_D} \frac{\|\mathbf{w}_{2,i}\|^2}{\epsilon} \leq P_H + (1-\alpha)P_{2,b}, \quad (9e)$$

$$0 < \alpha < 1, \quad (9f)$$

where $P_H = E_H/T$, and \bar{P}_b and \bar{P}_u denote the maximum transmit powers of the SBS and UL UE, respectively. Constraint (9b) ensures that each UL UE achieves the minimum specified data-rate of \bar{r}_j^U . Constraints (9c) and (9d) represent the restrictions on the maximum transmit powers of the SBS and the UL UEs, respectively. Constraint (9e) restricts the SBS to use the harvested SEg in the second phase, if it is sufficient; otherwise, the SBS draws the energy from the grid source to sustain the transmissions. Evidently, (9) is a nonconvex problem and obtaining an optimal solution is challenging and converges slowly. Hence, we seek a rapidly converging suboptimal solution in the following section.

IV. PROPOSED SOLUTION METHOD

There are two main steps involved to arrive at the rapidly converging solution. In the *first step*, we perform a few equivalent transformations on (9), similar to [9] and [11], to expose the hidden convexity and gain tractability. Accordingly, the resulting problem is expressed equivalently as

$$\max_{\Xi} q^2 \quad (10a)$$

$$\text{s.t. } z_j^U \geq \bar{r}_j^U \quad \forall j \in \mathcal{U}, \quad (10b)$$

$$(\mathbf{1}^T \mathbf{z}_1^D + \mathbf{1}^T \mathbf{z}_2^D + \mathbf{1}^T \mathbf{z}^U) \tau \geq q^2 \quad (10c)$$

$$\frac{1}{c} \geq \sum_{i=1}^{K_D} \frac{\|\mathbf{w}_{1,i}\|^2}{\epsilon} + P_b^{\text{cir}} + \frac{P_{2,b}}{\alpha} - p_{2,b} + \sum_{j=1}^{K_U} \left(p_{1,j} + \frac{p_{2,j}}{\alpha} - p_{2,j} \right) \quad (10d)$$

$$c \geq \alpha \tau \quad (10e)$$

$$\frac{|\mathbf{h}_i^H \mathbf{w}_{1,i}|^2}{u_{1,i}^D} \geq \sigma_i^2 + \sum_{k \neq i}^{K_D} |\mathbf{h}_i^H \mathbf{w}_{1,k}|^2 + \sum_{j=1}^{K_U} p_{1,j} |g_{j,i}|^2 \quad \forall i \in \mathcal{D}, \quad (10f)$$

$$\mathbf{h}_i^H \mathbf{W}_{2,i} \mathbf{h}_i \geq u_{2,i}^D b_i \quad \forall i \in \mathcal{D}, \quad (10g)$$

$$u_{1,i}^D + 1 \geq (t_{1,i}^D)^{1/\alpha}, \quad u_{2,i}^D + 1 \geq (t_{2,i}^D)^{1/(1-\alpha)} \quad \forall i \in \mathcal{D}, \quad (10h)$$

$$b_i \geq \sigma_i^2 + \sum_{k \neq i}^{K_D} \mathbf{h}_i^H \mathbf{W}_{2,k} \mathbf{h}_i + \sum_{j=1}^{K_U} p_{2,j} |g_{j,i}|^2 \quad \forall i \in \mathcal{D}, \quad (10i)$$

$$x_j^2 \mathbf{g}_j^H \mathbf{X}^{-1} \mathbf{g}_j \geq u_j^U \quad \forall j \in \mathcal{U}, \quad (10j)$$

$$u_j^U + 1 \geq (t_j^U)^{1/(1-\alpha)} \quad \forall j \in \mathcal{U}, \quad (10k)$$

$$p_{2,j} \geq x_j^2 \quad \forall j \in \mathcal{U}, \quad (10l)$$

$$t_{1,i}^D \geq e^{z_{1,i}^D}, \quad t_{2,i}^D \geq e^{z_{2,i}^D}, \quad t_j^U \geq e^{z_j^U} \quad \forall (i, j) \in (\mathcal{D}, \mathcal{U}), \quad (10m)$$

$$\eta \bar{P}_H \geq \frac{P_b^{\text{cir}}}{\alpha} - P_b^{\text{cir}} + \sum_{j=1}^{K_U} \beta_j \left(\frac{z_j^U}{\alpha} - z_j^U \right) - \frac{P_{2,b}}{\alpha} + p_{2,b} + \frac{1}{\epsilon} \sum_{i=1}^{K_D} \frac{\text{tr}(\mathbf{W}_{2,i})}{\alpha} - \text{tr}(\mathbf{W}_{2,i}), \quad (10n)$$

$$\frac{\bar{P}_b}{\alpha} \geq \sum_{i=1}^{K_D} \left(\|\mathbf{w}_{1,i}\|^2 + \frac{\text{tr}(\mathbf{W}_{2,i})}{\alpha} - \text{tr}(\mathbf{W}_{2,i}) \right), \quad (10a)$$

$$\frac{\bar{P}_u}{\alpha} \geq p_{1,j} + \frac{p_{2,j}}{\alpha} - p_{2,j} \quad \forall j \in \mathcal{U}, \quad (10p)$$

$$(9f), \quad (10q)$$

$$\text{rank}(\mathbf{W}_{2,i}) = 1, \quad \forall i \in \mathcal{D}, \quad (10r)$$

where $\bar{P}_H \triangleq P_H/\alpha$ and $\mathbf{W}_{2,i} = \mathbf{w}_{2,i}\mathbf{w}_{2,i}^H$ is a rank-1 positive semi-definite (PSD) matrix. The introduction of $\mathbf{W}_{2,i}$ helps convexify (10j) [11], which is otherwise a difficult constraint to handle. For notational compactness, a set $\Xi = \{\mathbf{w}, \mathbf{W}, \mathbf{p}, \alpha, \mathbf{z}, \mathbf{u}, \mathbf{t}, \mathbf{b}, \mathbf{x}, c, \tau, q\}$ is introduced, which collects all the optimization variables, where $\mathbf{w}_{\geq 0}, \mathbf{z}_{\geq 0}, \mathbf{u}_{\geq 0}, \mathbf{t}_{\geq 1}$ collect $\{\mathbf{W}_{2,1}, \dots, \mathbf{W}_{2,K_D}\}, \{\mathbf{z}_1^D, \mathbf{z}_2^D, \mathbf{z}^U\}, \{\mathbf{u}_1^D, \mathbf{u}_2^D, \mathbf{u}^U\}$ and $\{\mathbf{t}_1^D, \mathbf{t}_2^D, \mathbf{t}^U\}$, respectively. $\mathbf{z}_1^D = [z_{1,1}^D, \dots, z_{1,K_D}^D]^T, \mathbf{z}_2^D = [z_{2,1}^D, \dots, z_{2,K_D}^D]^T, \mathbf{z}^U = [z^U, \dots, z_{K_D}^U]^T, \mathbf{u}_1^D \in \{u_{1,1}^D, \dots, u_{1,K_D}^D\}, \mathbf{u}_2^D \in \{u_{2,1}^D, \dots, u_{2,K_D}^D\}, \mathbf{u}^U \in \{u^U, \dots, u_{K_D}^U\}, \mathbf{t}_1^D \in \{t_{1,1}^D, \dots, t_{1,K_D}^D\}, \mathbf{t}_2^D \in \{t_{2,1}^D, \dots, t_{2,K_D}^D\}, \mathbf{t}^U \in \{t^U, \dots, t_{K_D}^U\}, \mathbf{b} \in \{b_1, \dots, b_{K_D}\}, \mathbf{x} \in \{x_1, \dots, x_{K_D}\}, c \geq 0, \tau \geq 0, q \geq 0$ are slack variables. It is easy to see that a solution to (10) is also feasible for (9). Moreover, all the constraints (10b)-(10n) are active at optimality, and hence, (10) is an equivalent formulation of (9). Note that, to write (10c) as a second-order cone (SOC) constraint, we introduce q^2 in the objective function; however, its maximization is a nonconvex problem. Hence, we equivalently replace the objective function with q , which also maximizes q^2 . Next, to achieve further tractability, we relax the nonconvex rank-1 constraint (10r) by dropping it. Now, (10) can be equivalently expressed as

$$\max_{\Xi} \{q | (10b) - (10q)\}. \quad (11)$$

In the *second step*, we identify the nonconvex parts of (11) and linearize them with a first-order Taylor approximation around the point of operation [12]. This step leads to an iterative procedure and a local solution to (11). In (10), the constraints (10d)-(10h), (10k), (10n)-(10p) are nonconvex. Particularly, the nonconvexity in (10d), (10f), (11) and (10p) is due to the convex function of form $f_1(x, y) = |x|^2/y, \forall x \in \mathbb{C}^N, y \in \mathbb{R}^+$, on the greater side of the inequalities. Functions of this form can be approximated, around a point $(x^{(n)}, y^{(n)})$ at the n th iteration, as $F_1^{(n)}(x, y) = 2\Re(x^{(n)}x)/y^{(n)} - |x^{(n)}|^2 y^{(n)}/(y^{(n)})^2$. The constraints (10d), (10h), (10k), (10n), (11) and (10p) also have nonconvexity due the presence of functions of the forms $f_2(x, y) = x/y$ and $f_3(x, y) = x^{(1/y)}, \forall x \in \mathbb{C}^N, y \in (0, 1)$, which we linearize around a point $x^{(n)}, y^{(n)}$, as $F_k^{(n)}(x, y) = f_k(x^{(n)}, y^{(n)}) + \langle \nabla f_k(x^{(n)}, y^{(n)}), (x, y) - (x^{(n)}, y^{(n)}) \rangle, k \in \{2, 3\}$ [13]. The constraints (10e) and (10g) have nonconvexity on the lesser side of the inequalities of the form $f_4(x, y) = xy, \forall x \in \mathbb{C}^N, y \in \mathbb{R}^+$. Using the result from [14], we replace $f_4(x, y)$ with its convex upper bound around a point $(x^{(n)}, y^{(n)})$ as $F_4^{(n)}(x, y, \phi^{(n)}) = 0.5(\phi^{(n)}(x^{(n)})^2 + (y^{(n)})^2/\phi^{(n)}), \forall \phi^{(n)} = y^{(n)}/x^{(n)} > 0$. The approximations employed above satisfy the following three conditions [12]: i) $F^{(n)}(x) \leq f(x), \forall x$; ii) $F^{(n)}(x^{(n-1)}) = f(x^{(n-1)})$; iii) $\nabla F^{(n)}(x^{(n-1)}) = \nabla f(x^{(n-1)})$, and hence, the convergence of the iterative procedure is ensured. Now, by replacing the nonconvex parts of the constraints with the approximations discussed above, (11) can be formulated as a convex problem at the n th iteration as

$$\max_{\Xi} q \quad (12a)$$

$$\text{s.t. } F_1^{(n)}(1, c) \geq \sum_{i=1}^{K_D} \|\mathbf{w}_{1,i}\|^2 + P_b^{\text{cir}} + F_2^{(n)}(\alpha, p_{2,b}) - p_{2,b} + \sum_{j=1}^{K_U} (p_{1,j} + F_2^{(n)}(\alpha, p_{2,j}) - p_{2,j}) \quad (12b)$$

$$c \geq F_4^{(n)}(\alpha, \tau, \phi_1^{(n)}) \quad (12c)$$

$$F_1^{(n)}(\mathbf{w}_{1,i}, u_{1,i}^D) \geq \sigma_i^2 + \sum_{k \neq i}^{K_D} |\mathbf{h}_i^H \mathbf{w}_{1,k}|^2 + \sum_{j=1}^{K_U} p_{1,j} |g_{j,i}|^2 \quad \forall i \in \mathcal{D}, \quad (12d)$$

$$\mathbf{h}_i^H \mathbf{W}_{2,i} \mathbf{h}_i \geq F_4^{(n)}(u_{2,i}^D, b_i, \phi_{2,i}^{(n)}) \quad \forall i \in \mathcal{D}, \quad (12e)$$

$$u_{1,i}^D + 1 \geq F_3^{(n)}(t_{1,i}^D, \alpha), u_{2,i}^D + 1 \geq F_3^{(n)}(t_{2,i}^D, \bar{\alpha}) \quad \forall i \in \mathcal{D}, \quad (12f)$$

$$u_j^U + 1 \geq F_3^{(n)}(t_j^U, \bar{\alpha}) \quad \forall j \in \mathcal{U}, \quad (12g)$$

$$\eta \bar{P}_H \geq \frac{\bar{\alpha} P_b^{\text{cir}}}{\alpha} + \sum_{j=1}^{K_U} \beta_j (F_2^{(n)}(\alpha, z_j^U) - z_j^U) - F_2^{(n)}(\alpha, p_{2,b}) + p_{2,b} + \frac{1}{\epsilon} \sum_{i=1}^{K_D} F_2^{(n)}(\alpha, \text{tr}(\mathbf{W}_{2,i})) - \text{tr}(\mathbf{W}_{2,i}), \quad (12h)$$

$$\frac{\bar{P}_b}{\alpha} \geq \sum_{i=1}^{K_D} \left(\|\mathbf{w}_{1,i}\|^2 + F_2^{(n)}(\alpha, \text{tr}(\mathbf{W}_{2,i})) - \text{tr}(\mathbf{W}_{2,i}) \right), \quad (12i)$$

$$\frac{\bar{P}_u}{\alpha} \geq p_{1,j} + F_2^{(n)}(\alpha, p_{2,j}) - p_{2,j} \quad \forall j \in \mathcal{U}, \quad (12j)$$

$$(10b), (10c), (10i), (10j), (10l), (10m), (9f), \quad (12k)$$

where $\bar{\alpha} \triangleq 1 - \alpha$. Pseudocode for solving (12) is outlined in Algorithm 1. Note that the constraints in (10m) are exponential cones, which we approximate as a set of SOC constraints [15], [16] in Algorithm 1. Since the problem is upper bounded due to power constraints, the algorithm generates a monotonic non-decreasing sequence of objective function values and converges

to a Karush-Kuhn-Tucker (KKT) point of (11) [12]. The detailed proof follows similar lines as the one discussed in [17], and hence, is omitted here for brevity.

The feasible initial point to Algorithm 1 is generated by solving the following problem; $\max_{\Xi, \mu \leq 0} \{q + \mathbf{1}^T \mu\} / \{(12b) - (12k)/(10b)\}$ subject to $\bar{r}_j^U + \mu_j \leq z_j^U \forall j \in \mathcal{U}$, where $\mu = [\mu_1, \dots, \mu_{K_U}]^T$ are the newly introduced variables. The feasible initial point is obtained when $\mu = \mathbf{0}$ and requires three iterations at most.

Algorithm 1 The proposed iterative algorithm	
Input:	$\mathbf{H}, \mathbf{H}_{\text{on}}, \mathbf{h}, \mathbf{g}, \sigma_n^2, P_b^{\text{cir}}, \bar{P}_b, \bar{P}_u, I_{\text{max}} = 400.$
Output:	$\mathbf{w}, \mathbf{p}, \alpha.$
1:	Initialize $\Xi^{(n)}$ and set $n := 0;$
2:	repeat
3:	Solve (12) for local optimal values of $\mathcal{X}^*;$
4:	Update $\Xi^{(n)} = \Xi^*, \phi_1^{(n)} = \tau^*/\alpha^*, \phi_{2,i}^{(n)} = b_{2,i}^{D*}/u_{2,i}^{D*}, \forall i \in \mathcal{D},$ and $n := n + 1;$
5:	until Convergence of the objective function or $n \geq I_{\text{max}}$
6:	Perform randomization to extract a rank-one solution [18].

TABLE I
SIMULATION PARAMETERS.

Parameters	Value
No. of antennas and cell radius	$M_T = 2, M_R = 2,$ and 100 m
Transmit and circuit powers (dBm)	$\bar{P}_b: 24, \bar{P}_u: 23, P_b^{\text{cir}}: 30$
β, η, ϵ	0.1, 0.5, 0.69
Bandwidth	10 MHz
Thermal noise density and SI	-174 dBm/Hz, $\sigma_{\text{SI}}^2 = -110$ dB
Noise figure [18]	SBS: 13 dB, UE: 9 dB
Path loss (in dB) UE-to-SBS where d is in km [18]	LOS: $103.8 + 20.9 \log_{10}(d)$ NLOS: $145.4 + 37.5 \log_{10}(d)$
Path loss (in dB) UE-to-UE where d is in km [18]	LOS: $98.5 + 20 \log_{10}(d)$ NLOS: $175.78 + 40 \log_{10}(d)$

V. NUMERICAL RESULTS

In this section, a performance evaluation of the proposed SEg harvesting scheme is presented. The parameters used in simulations with their values are listed in Table I. The algorithm is implemented using the CVX parser [20] and `mosek` as an internal solver. The minimum data-rate required for each UL UE is set to $\bar{r}_j^U = 1$ Mbit/s. A small cell of radius 100 m is considered with $K_D = K_U = 2$ uniformly distributed UEs within the cell area. The channels are Rayleigh faded with each coefficient following the $CN(0, 1)$ distribution. The SI channel is modeled as Rician, with Rician factor $K = 1$, i.e., $\mathbf{H}_{\text{on}} \sim CN_{M_T \times M_R} \left(\sqrt{\sigma_{\text{SI}}^2 K / (K + 1)} \bar{\mathbf{H}}, (\sigma_{\text{SI}}^2 / (1 + K)) \mathbf{I}_{M_R} \otimes \mathbf{I}_{M_T} \right)$, where $\bar{\mathbf{H}}$ is a deterministic matrix and \otimes denotes the Kronecker product. σ_{SI}^2 denotes the ratio of the average SI powers before and after the SIC. Results are obtained based on 1000 runs.

In Fig. 1, we show the convergence behavior of the iterative Algorithm 1. The objective function values are plotted versus the number of iterations for two independent random channels states and $\bar{P}_b = 25$ dBm. We observe that Algorithm 1 converges in less than fifty iterations for all three channel realizations. For benchmarking purpose, the objective function values are also compared with the global ones, which are obtained using the branch-reduce-and-bound algorithm [21].

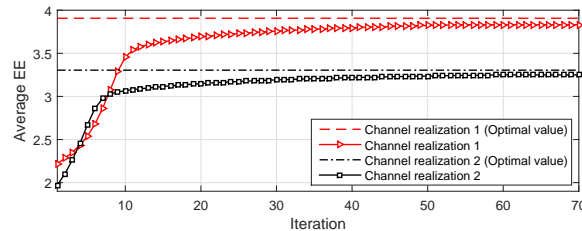


Fig. 1. Convergence behavior of Algorithm 1 for two independent channel realizations with $\bar{P}_b = 25$ dBm, $M_T = 1$, and $M_R = 1$.

In Fig. 2, the average EE (AEE) with and without the SEg harvesting scheme versus the transmit power of the SBS is plotted. It can be seen that the average gain of the scheme that harvests SEg is significantly higher than the one that does not harvest. The AEE of both schemes saturates in the high \bar{P}_b regime; however, the former saturates later than the latter. In low-power regime, for the proposed scheme, the SBS harvests less SEg and draws more energy from the grid source for decoding the UL users data, and hence, the AEE drops. Note that the AEE of the latter is obtained by using Algorithm 1 with

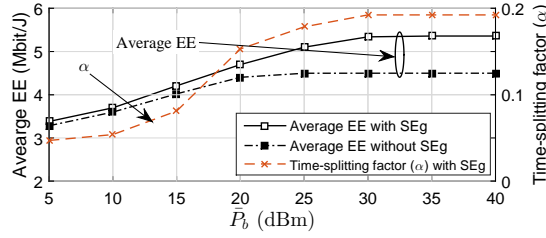


Fig. 2. The average EE (left-hand side y-axis) and the time-splitting factor (right-hand side y-axis) versus the maximum transmit power of the SBS.

fixed $\alpha = 0$. The time-splitting factor α is also shown on the right-hand side y-axis of the figure. Its values increase with \bar{P}_b but saturates in the high \bar{P}_b regime.

Lastly, we have observed that in the first phase Algorithm 1 allocates zero power to each UL UE for all values of \bar{P}_b , and accordingly, the SBS harvests only the SEg.

VI. CONCLUSION

We have considered a FD SBS, in which, by installing an additional on and off SIC switch, the FD SBS can harvest SEg from the SI. The SEg is harvested when the SIC switch is off; otherwise, there is no harvesting. The fraction of the transmission time for which the SIC switch is on has been investigated jointly with the beamformer and power allocations that maximize the EE of the SBS. Numerical results have shown that significant AEE gain is attained by the system that allows SEg harvesting.

REFERENCES

- [1] W. Li *et al.*, "System scenarios and technical requirements for full-duplex concept," DUPLO Deliverable D1.1., Tech. Rep., Apr. 2013.
- [2] S. Bi, C. K. Ho, and R. Zhang, "Wireless powered communication: Opportunities and challenges," *IEEE Commun. Mag.*, vol. 53, no. 4, pp. 117–125, Apr. 2015.
- [3] C. Zhong *et al.*, "Wireless information and power transfer with full duplex relaying," *IEEE Trans. Commun.*, vol. 62, no. 10, pp. 3447–3461, Oct. 2014.
- [4] V. D. Nguyen, T. Q. Duong, H. D. Tuan, O. S. Shin, and H. V. Poor, "Spectral and energy efficiencies in full-duplex wireless information and power transfer," *IEEE Trans. Commun.*, vol. 65, no. 5, pp. 2220–2233, May 2017.
- [5] Y. Zeng and R. Zhang, "Full-duplex wireless-powered relay with self-energy recycling," *IEEE Commun. Lett.*, vol. 4, no. 2, pp. 201–204, Apr. 2015.
- [6] D. Hwang, K. C. Hwang, D. I. Kim, and T. J. Lee, "Self-energy recycling for RF powered multi-antenna relay channels," *IEEE Trans. Wireless Commun.*, vol. 16, no. 2, pp. 812–824, Feb. 2017.
- [7] M. Maso, C. F. Liu, C. H. Lee, T. Q. S. Quek, and L. S. Cardoso, "Energy-recycling full-duplex radios for next-generation networks," *IEEE J. Select. Areas Commun.*, vol. 33, no. 12, pp. 2948–2962, Dec. 2015.
- [8] S. Cui, A. Goldsmith, and A. Bahai, "Energy-efficiency of MIMO and cooperative MIMO techniques in sensor networks," *IEEE J. Select. Areas Commun.*, vol. 22, no. 6, pp. 1089–1098, Aug. 2004.
- [9] A. Yadav, O. A. Dobre, and N. Ansari, "Energy and traffic aware full-duplex communications for 5G systems," *IEEE Access*, vol. 5, pp. 11 278–11 290, May 2017.
- [10] A. Zappone, L. Sanguinetti, G. Bacci, E. Jorswieck, and M. Debbah, "Energy-efficient power control: A look at 5G wireless technologies," *IEEE Trans. Signal Processing*, vol. 64, no. 7, pp. 1668–1683, Apr. 2016.
- [11] D. Nguyen, L. N. Tran, P. Pirinen, and M. Latva-aho, "On the spectral efficiency of full-duplex small cell wireless systems," *IEEE Trans. Wireless Commun.*, vol. 13, no. 9, pp. 4896–4910, Sep. 2014.
- [12] B. R. Marks and G. P. Wright, "A general inner approximation algorithm for nonconvex mathematical programs," *Oper. Res.*, vol. 26, no. 4, pp. 681–683, Aug. 1978.
- [13] H. Tuy, *Convex Analysis and Global Optimization*, 2nd ed. Springer, 2016.
- [14] L. N. Tran, M. F. Hanif, A. Tölli, and M. Juntti, "Fast converging algorithm for weighted sum rate maximization in multicell MISO downlink," *IEEE Signal Processing Lett.*, vol. 19, no. 12, pp. 872–875, Dec. 2012.
- [15] A. Ben-Tal and A. Nemirovski, "On polyhedral approximations of the second-order cone," *Math. Operat. Res.*, vol. 26, no. 2, pp. 19–205, May 2001.
- [16] T. M. Nguyen, A. Yadav, W. Ajib, and C. Assi, "Resource allocation in two-tier wireless backhaul heterogeneous networks," *IEEE Trans. Wireless Commun.*, vol. 15, no. 10, pp. 6690–6704, Oct. 2016.
- [17] —, "Centralized and distributed energy efficiency designs in wireless backhaul HetNets," *IEEE Trans. Wireless Commun.*, vol. 16, no. 7, pp. 4711–4726, Jul. 2017.
- [18] N. D. Sidiropoulos, T. N. Davidson, and Z.-Q. Luo, "Transmit beamforming for physical-layer multicasting," *IEEE Trans. Signal Processing*, vol. 54, no. 6, pp. 2239–2251, Jun. 2006.
- [19] "Further enhancements to LTE time division duplex (TDD) for downlink-uplink (DL-UL) interference management and traffic adaptation," 3GPP, TR 36.828, v.11.0.0., Tech. Rep., Jun. 2012.
- [20] M. Grant and S. Boyd, "CVX: Matlab software for disciplined convex programming, version 2.1," <http://cvxr.com/cvx>, Mar. 2014.
- [21] E. Björnson, G. Zheng, M. Bengtsson, and B. Ottersten, "Robust monotonic optimization framework for multicell MISO systems," *IEEE Trans. Signal Processing*, vol. 60, no. 5, pp.2508–2523, May 2012.